Conference Paper, Published Version

Stelzer, Oliver; Schwab, Radu; Neumann, Sven

Geotechnical Measurements during Construction and Operation of Sülfeld lock

Geotechnical Measurements during Construction and Operation of Sülfeld lock

Oliver Stelzer, Radu Schwab
Federal Waterways Engineering and Research Institute (BAW), Karlsruhe, Germany

Sven Neumann
Mittelland Canal Construction Office (NBA), Hannover, Germany

1 Introduction

The Sülfeld Lock is situated at approx. 6 km to the west of Wolfsburg and covers a difference in altitude of 9 m between the summit reach and the eastern reach of the Mittelland Canal. The facility, which was put into operation in 1938, consists of a twin lock with 6 fan-shaped water-saving basins for each lock (Fig. 1).

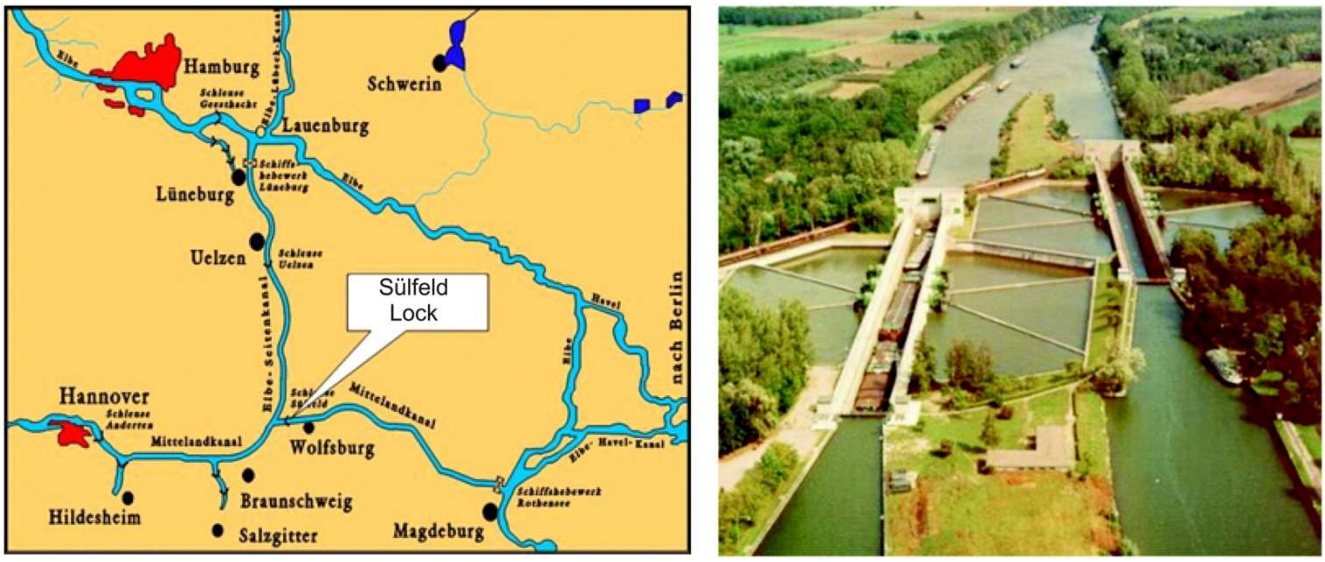

Figure 1: Geographical situation and aerial photograph of the Süldfeld Lock prior to the new construction

Within the context of the Mittelland Canal development, the Sülfeld Lock was adapted to the demands of modern freight shipping. For this purpose, the southern lock chamber, which was in a poorer structural state than the northern lock, was demolished as well as

the adjoined water-saving basins and replaced by a new lock. The new lock has been in operation since November 2008.

2 Description of the new lock

The new lock was designed as a single-chamber lock with two open, terraced water-saving basins (Fig. 2). The operational length of the lock is 225 m and the width is 12.50 m.

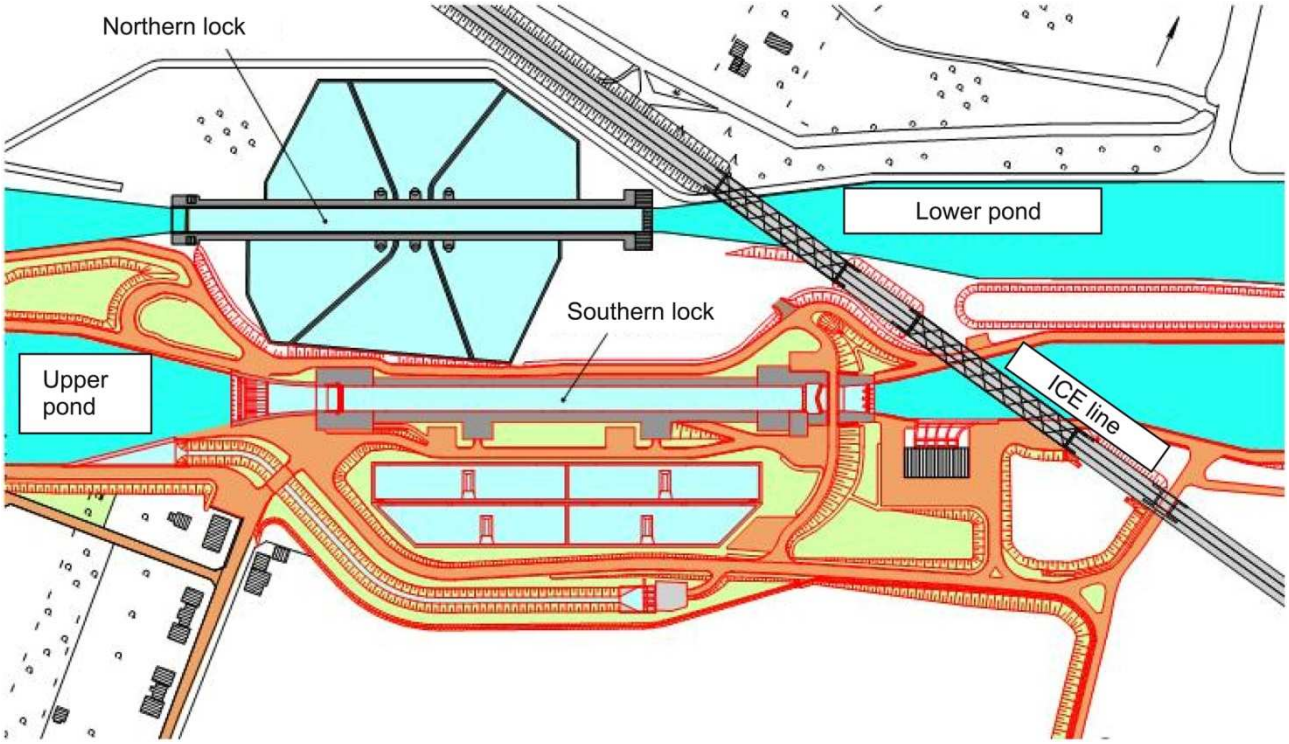

Figure 2: Site plan of the new southern lock

The lock chamber was designed as an open U-frame and implemented as a solid construction on a raft footing at approx. 46 m above sea level (a.s.l.), i.e. 20 m below the natural terrain in the area at the upper lock gate. The foundation level is mostly situated in a glacial till layer. A monolithic base slab was implemented, while the chamber walls were divided into individual blocks with a length of up to 45 m. The advantage of the monolithic construction, as opposed to a construction including joints, is the reduction of varying settlement levels among neighbouring blocks. The lock floor is 5 m thick with an integrated 2 m high and 9.50 m wide longitudinal culvert filling system. The thickness of the chamber walls is 2.50 m throughout the entire structure.

3 Ground and groundwater conditions

Comprehensive site investigation detected the following soil profile (Fig. 3):

- upper sands/backfill, thickness up to 10 m,
- glacial till (partially with sand pockets), thickness up to 20 m,
- lower sands,
- basin silt, thickness up to 10 m,
- rock (marl- and claystone).

The glacial till layer and the layers below are overconsolidated due to glacial loading. In the rock, a fracture zone is located in a SE-NW direction. The fault-line separates marl and claystone rock masses.

Aquifers can be found in three layers, which are separated from each other by aquicludes. The unconfined aquifer of the upper sands is separated from the confined aquifer of the lower sands by a thick, low permeable glacial till layer. The separating layer between the lower sands and the rock layer aquifer, which exists almost throughout the entire examined site, consists of low permeable basin silt.

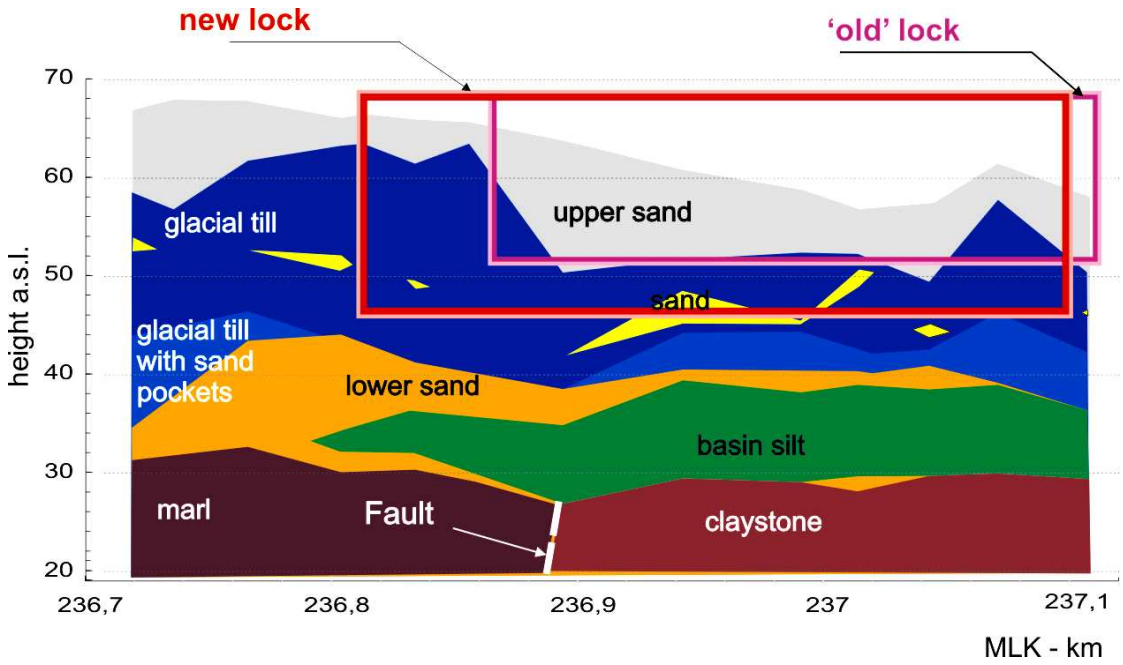

Figure 3: Longitudinal section and soil profile

4 Construction pit

The construction of the new lock required a concept for the construction pit [1] which ensures a safe and economic implementation under the given geotechnical conditions. Moreover, the influence of the new lock's construction on neighbouring structures (water-saving basins of the northern lock, a pump house and the bridge abutment of the high-speed railway Hannover-Berlin) had to be examined (Fig. 4). Thus, for the concept of the construction pit, two demands were crucial:

- no large-scale lowering of the groundwater in the upper aquifer due to ecological reasons and due to possible settlements which would be harmful to the northern lock and its water-saving basins and
- a stiff construction to avoid unacceptable deformation of the neighbouring structures.

Figure 4: Location of the neighbouring structures

The above mentioned aspects taken into consideration, the retaining wall illustrated in Fig. 5 was selected. The following construction elements were applied: In the area of the neighbouring structures, which are prone to settlements, a diaphragm wall with up to nine rows of ground anchors was selected as well as a braced diaphragm wall at the area of the railway bridge. In the remaining areas, a cut-off wall was installed which, according to static requirements, was reinforced by an anchored sheet pile wall.

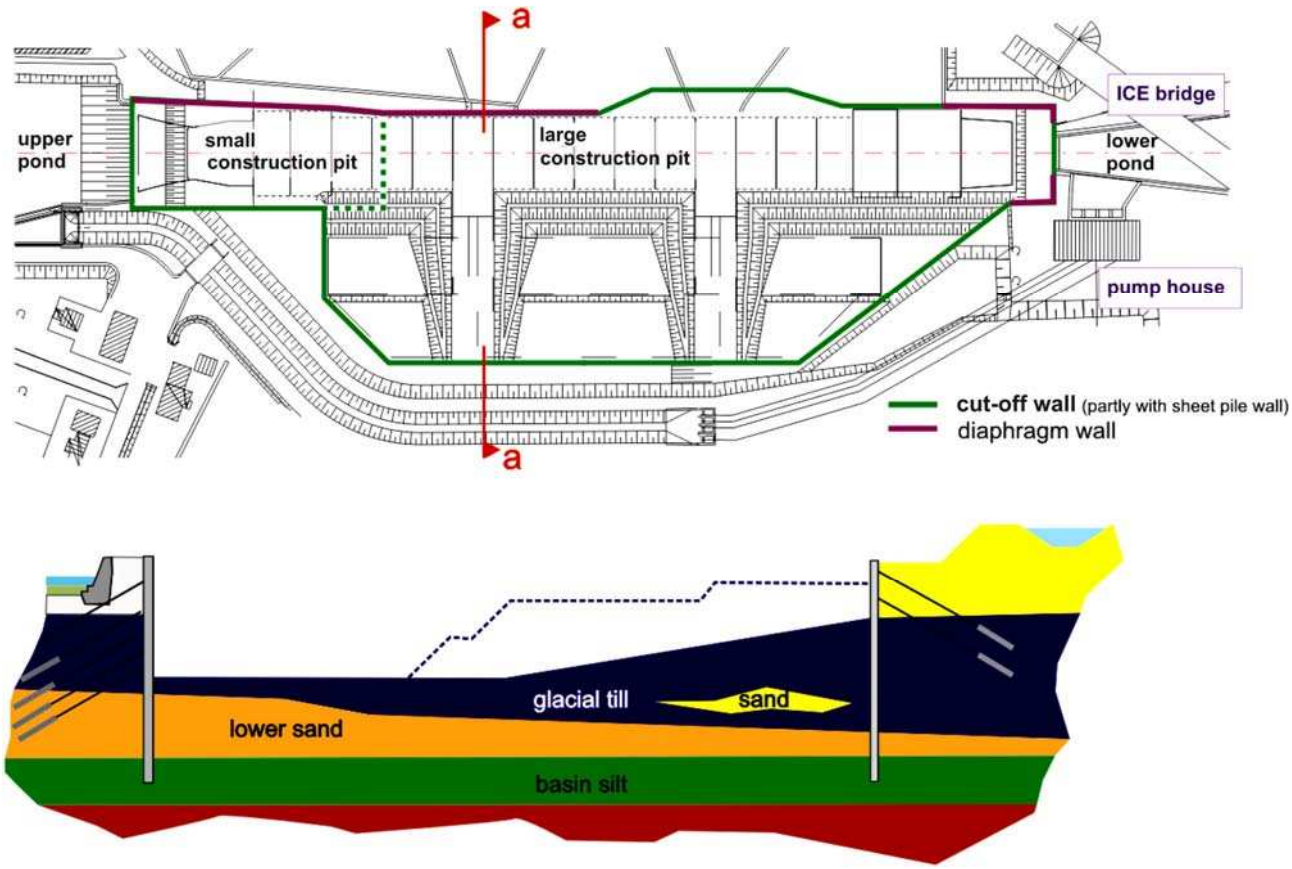

Figure 5: Retaining wall marked in the site plan and cross section a-a

Inside the pit wall, relief wells were installed in the lower sands and in the rock layer to obtain groundwater relief and thus protect the pit bottom from uplift. The pit bottom did not need to be sealed since the cut-off walls were driven down into the rock layer or into the low permeable basin silt layer. Lateral groundwater inflow could thus be excluded.

5 Measuring concept

When the geotechnical measuring concept was designed the following objectives were to be met:

- collection of evidence on the behaviour of neighbouring structures,
- monitoring of retaining walls and pit bottom deformation,
- development of a data basis for the calibration of finite element analyses during the construction phase,
- beyond the construction phase: monitoring of the structure’s behaviour (earth pressure, settlements, deformation of the chamber wall).

Measurements were performed in a total of seven cross sections: 3 main cross sections (HQ) and 4 secondary cross sections (NQ) (Fig. 6).

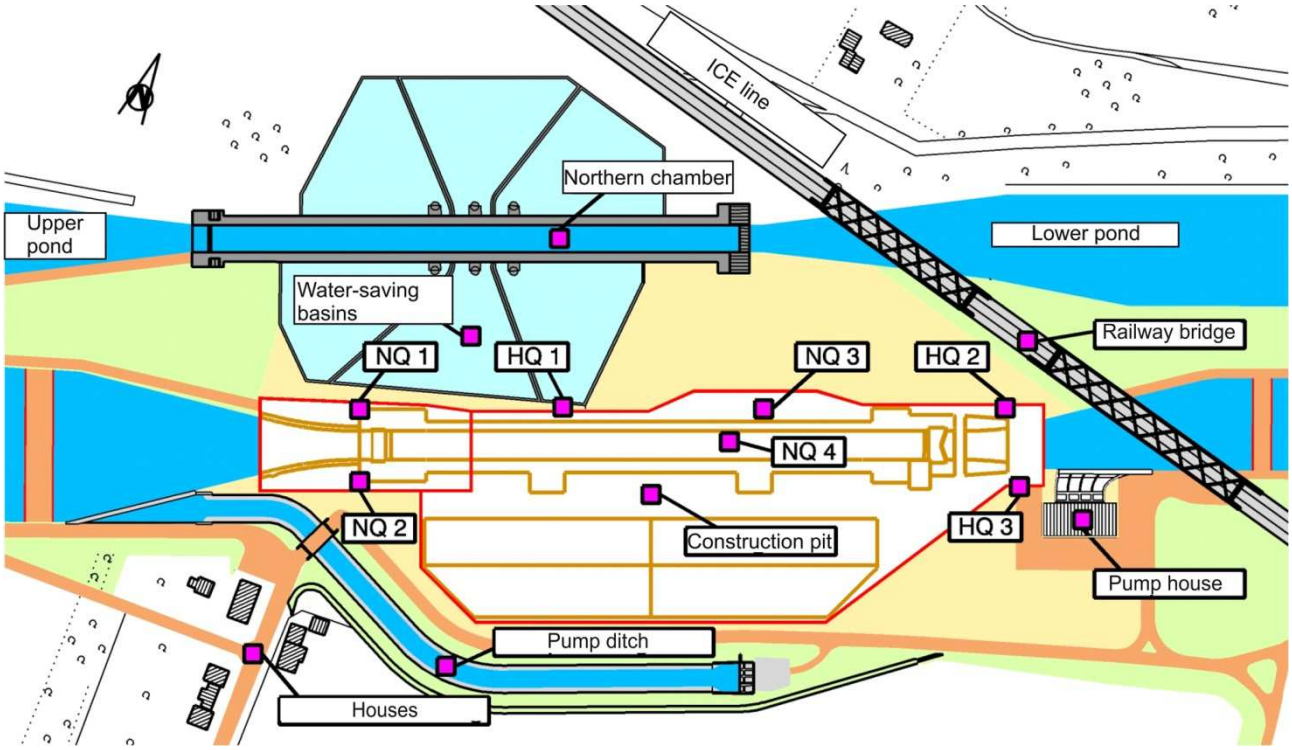

Figure 6: Site plan with instrumented cross sections

Table 1 presents the structures which were to be observed during the construction phases as well as the measurements at the retaining walls and the newly constructed lock. Furthermore, geodetic measurements and water level measurements were performed in the surroundings of the construction site.

The values measured by the transducers were automatically processed by data loggers in defined measuring intervals of 0.5 to 6 hours. They were transmitted via optical fibre cable, GSM connections or directional radio signals to a computer network in the observation division of the Mittelland Canal Construction Office in Hannover where they were compiled in a central database and made accessible to the participants of the project via internet (Fig. 7). More details on the topic of data collection can be found in [2].

Table 1: Overview of the observed objects and measurements

	Object	Parameters/critical effects	Measuring system
Monitoring of existent structures	Pump house	Inclination Settlements	Hydraulic levelling system Extensometer, geodesy
	Abutment of railway bridge	Horizontal deformation Settlements	Inverted pendulum Extensometer, geodesy
	Water-saving basins of the northern lock	Horizontal deformation	Geodesy
	Domain between water-saving basins and construction pit	Deformation	Inclinometer Pore pressure transducers Extensometer
Construction pit	Diaphragm wall	Horizontal deformation	Inclinometer, geodesy (HQ 1-3, NQ 1-3)
	Anchors	Anchor forces	Load cells (HQ 1, NQ 1-3)
	Struts	Strut forces	Load cells (HQ 2-3)
	Bottom of excavation	Heave Groundwater level	Extensometer (NQ 4) Pore pressure transducers
Lock	Bottom of lock chamber	Settlements	Extensometer (NQ 4), geodesy
	Chamber wall	Earth- and water pressure Horizontal deformation	Earth pressure cells and pore pressure transducers (close to NQ 3/4) Geodesy

With respect to evidence collection, the procedure was comprehensively documented. Apart from object-related measurement analyses, documentation efforts involved the composition of a monthly report on all object- and construction states.

A three-level reaction concept was designed for the project. Three reaction values for the relevant measuring parameters were defined based on the results of finite element predictions. By means of comparison with the measured values approaching or exceeding the prediction (level 1), the announcement of abnormal behaviour (level 2) and the approaching failure of the structure (level 3) could be automatically checked and reported. Whereas level 1 only resulted in increased attention according to this concept, level 2 reports had to be assessed and investigated immediately. For level 3 reports, an emergency plan was developed. In case of an emergency, amongst other measures, the high-speed railway could have been closed down any time.

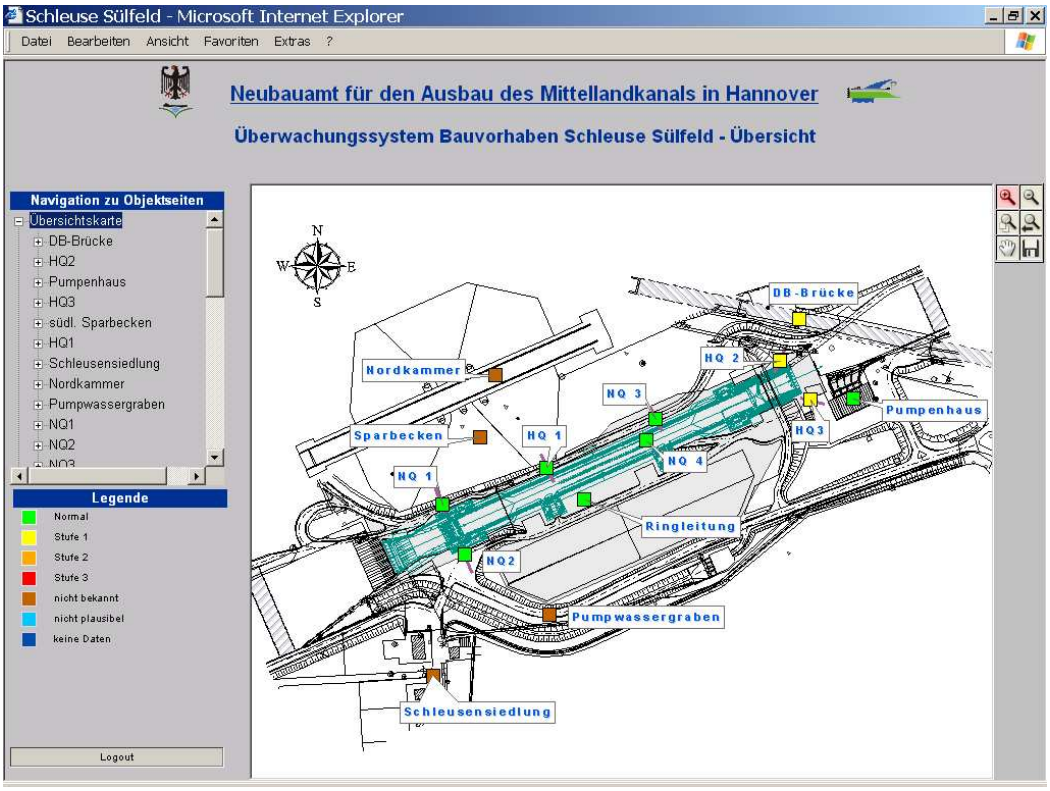

Figure 7: Overview of the homepage for the visualisation of the measuring results

6 Finite element calculations

Possible influences on the neighbouring structures had been analysed by the BAW (German Federal Waterways Engineering and Research Institute) through 2D and 3D finite element calculations starting early in the design stage. The railway bridges, the pumping station and the water-saving basins of the northern lock were integrated into finite element models to assess the interactions between these structures and the excavation for the new lock. After comparing the deformation predictions with the limit states of the neighbouring structures, a concept was finally selected for the construction pit which ensured sufficient safety.

During the construction phase, the actual movements were observed. The calibration of the finite element models allowed the verification and recalculation of the deformation predictions with increased precision. Moreover, values approaching the deformation limit states had to be recognised quickly enough to perform necessary construction measures.

This paper focuses on the analysis and recalculation of cross sections NQ 3 and NQ 4 (Fig. 8), the results being illustrated in chapter 7. The soil parameters calibrated during the

construction phase generated good results in the recalculation process and needed no further adaption.

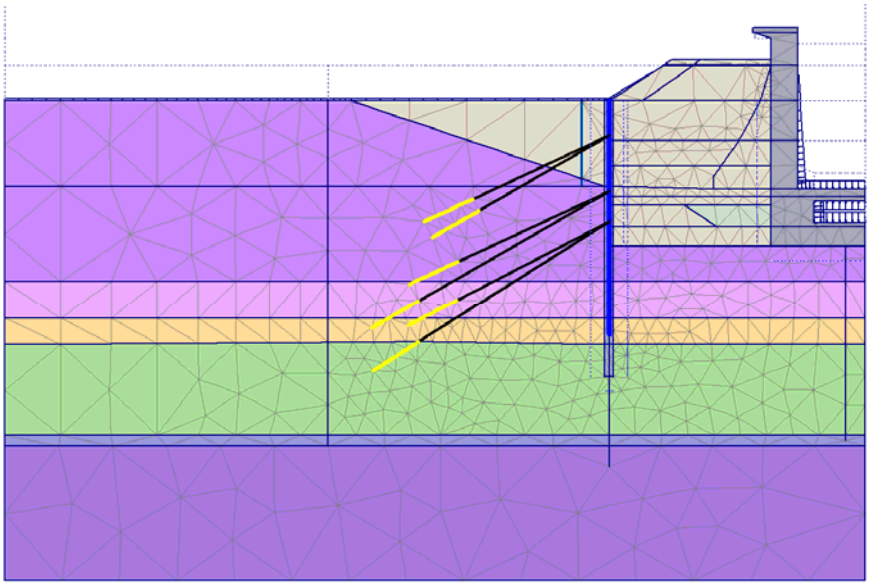

Figure 8: FEM model in the area of NQ 3 and NQ 4

7 Selected measuring results and comparison with finite element prognoses

In the following, some selected measuring results for the bridge abutment, different areas of the construction pit, and the finished lock will be illustrated and discussed.

7.1 Bridge abutment

Horizontal deformation of the bridge abutment closest to the construction pit was measured with an inverted pendulum attached to the abutment. Vertical deformation was measured with a pair of extensometers. Horizontal deformation of the bridge abutment after the excavation of the construction pit including the lower pond and after the removal of the struts amounts to 8-9 mm in direction of the construction pit (Fig. 9). At the same time, a settlement of 5 mm was observed. Supplementary geodetic measurements showed no tilting of the abutment.

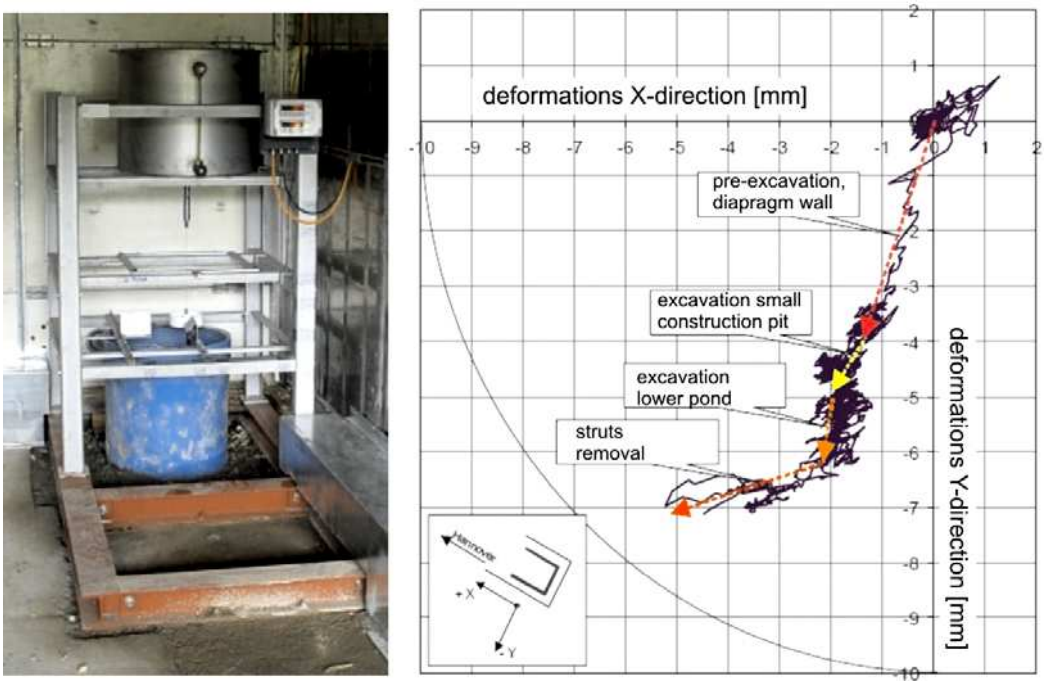

Figure 9: Inverted pendulum and plotted measuring results

The deformation of the bridge abutment and its recalculation with a 3D FEM model is presented in [3, 4]. The influence of different constitutive laws was estimated comparing the calculated results with the measurements. The closest approximation to the measured values was obtained using the hardening soil model (HS) with small-strain stiffness (HSsmall). Fig. 10 shows (as an example) a comparison of the horizontal deformation of the bridge abutments (after the excavation of the construction pit).

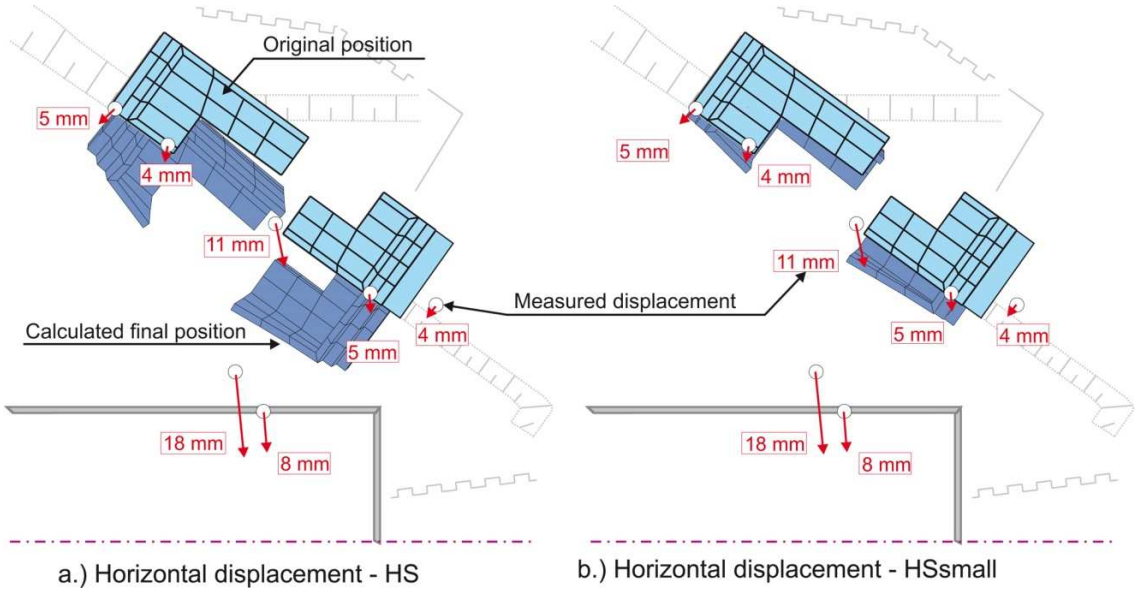

Figure 10: Measured and calculated horizontal deformation of the bridge abutments

To minimize the abutment's deformation due to the excavation, the construction pit was braced in this area. The strut forces measured for the struts S2, S3 and S6 are illustrated in the timeline in Fig. 11. For the longest strut S6, the impact of daily and seasonal temperature changes was particularly significant. Thanks to the insulation of this strut, daily strut force changes could almost be completely eliminated.

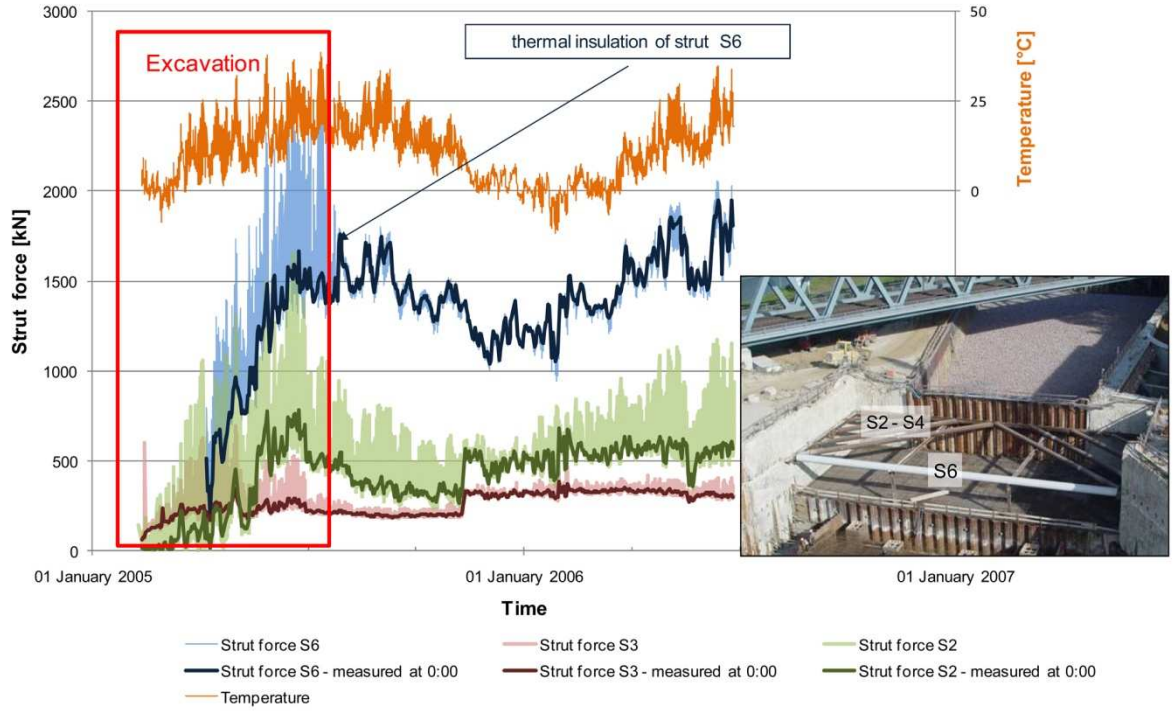

Figure 11: Measured strut forces in the sections HQ 2/3

7.2 Deformations of the construction pit and of the new lock

Horizontal deformation of the combined wall (cut-off wall reinforced by a sheet pile wall) at NQ 3 was measured in an inclinometer casing integrated into the wall. Fig. 12 shows the deformation measured after the completion of the excavation works. A maximum deformation of approx. 2.5 cm was recorded at the height of anchor row C. Unfortunately, the initial reading was performed after deformation had already occurred due to the excavation works and anchor pre-stressing. As the deformation history of the wall was incomplete, the measurement results obtained were difficult to interpret. To compare the measuring results with the results of the finite element analysis, several alternatives were developed for which the time of the initial reading was assumed either before or after pre-

stressing of anchor row A. These alternatives differ only above 51 m a.s.l. In fact, the initial reading was performed at one point during the pre-stressing of anchor row A. Thus, the mean value of both alternatives (solid red line in Fig. 12) corresponds well with the measurement. In addition, the calculated total deformation compared to the state prior to the construction works is plotted. The maximum deformation at the wall head is approx. 5 cm.

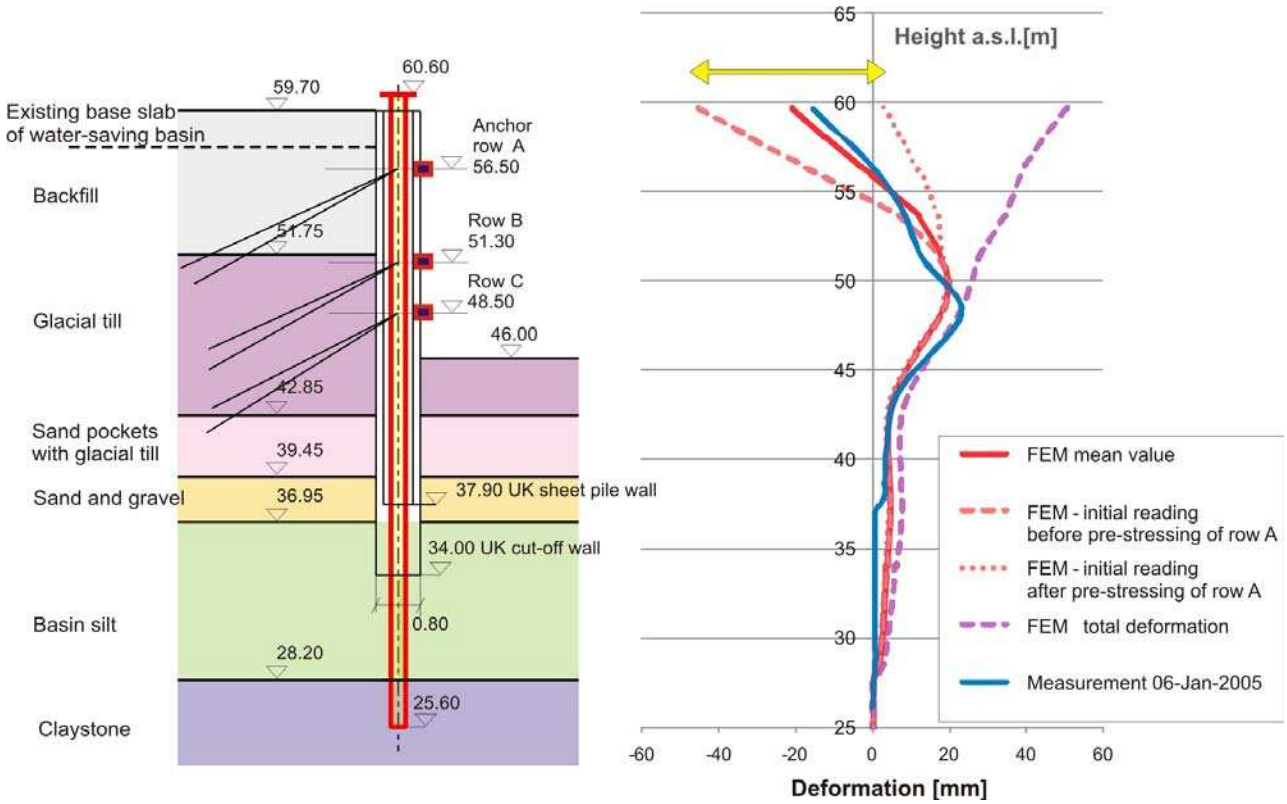

Figure 12: Soil profile, anchorage and inclinometer measurements at NQ 3

Vertical deformation of the bottom of the excavation pit was measured at NQ 4 with two multipoint rod extensometers. The results for the deepest anchor points at approx. 18 m below the pit bottom are illustrated in Fig. 13. As the extensometers had been installed before the excavation works started, heave of the pit bottom (maximum: approx. 2 cm by mid-2005) could be measured during the excavation phase as well as subsequent settlements (also approx. 2 cm by 2008) after the construction of the lock chamber and the backfilling behind the chamber walls. Then, a heave of approx. 5 mm occurred after the construction pit had no longer been dewatered and thus buoyant forces were acting at the lock. In autumn 2008, a first test flooding of the lock was performed. Operating the lock with permanently fluctuating water levels led to cyclical vertical deformation and additional

settlement of so far 4-5 mm. The red curve, which represents the deformation computed with finite element models, is close to the real behaviour. This required a consolidation analysis taking the construction process and the time of the individual construction phases into account. The differences in time evolution of deformations are mainly due to the quite simplified construction history used in the finite element simulation.

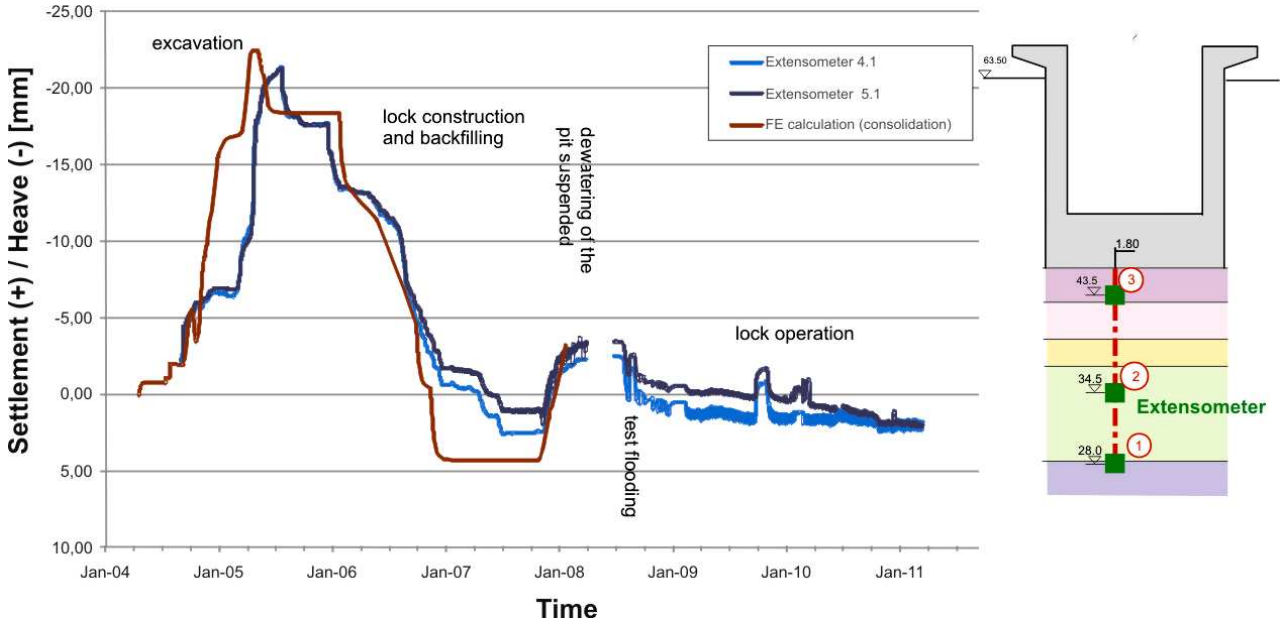

Figure 13: Vertical deformation of the pit bottom at NQ 4

7.3 Earth pressure

Close to NQ 4, earth pressure cells were installed at the back side of the lock chamber wall in three measuring levels at different heights (Fig. 15). For each measuring level, three earth pressure cells and one pore water transducer were installed (Fig. 14). Thus, effective earth pressure can be determined.

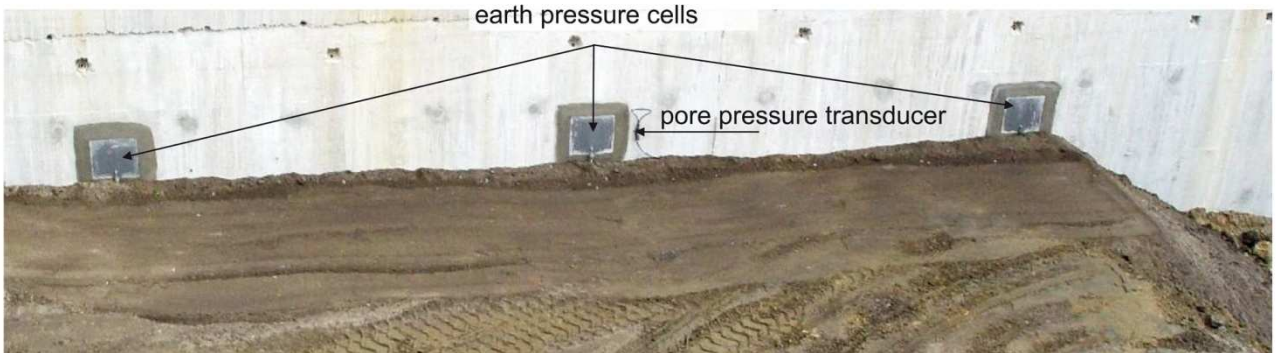

Figure 14: Installation of earth pressure cells

7.3.1 Temperature effects

Fig. 15 shows the earth pressure development at measuring levels 1 and 2 in 2007. At this time, the sand backfill behind the chamber wall close to the measuring instruments had already been completed but the lock had not yet been operational. The changes in earth pressure illustrated in Fig. 15 result from the deformation of the chamber wall due to temperature changes. In summer, the chamber wall becomes warmer at the side bordering the water than at the side bordering the soil. This causes the chamber wall to move towards the soil and thus the earth pressure to increase. In winter, the opposite can be observed: The wall moves away from the ground and the earth pressure decreases. The temperature's impact on earth pressure is particularly significant at measuring level 1 with more than 60 % with reference to the annual mean.

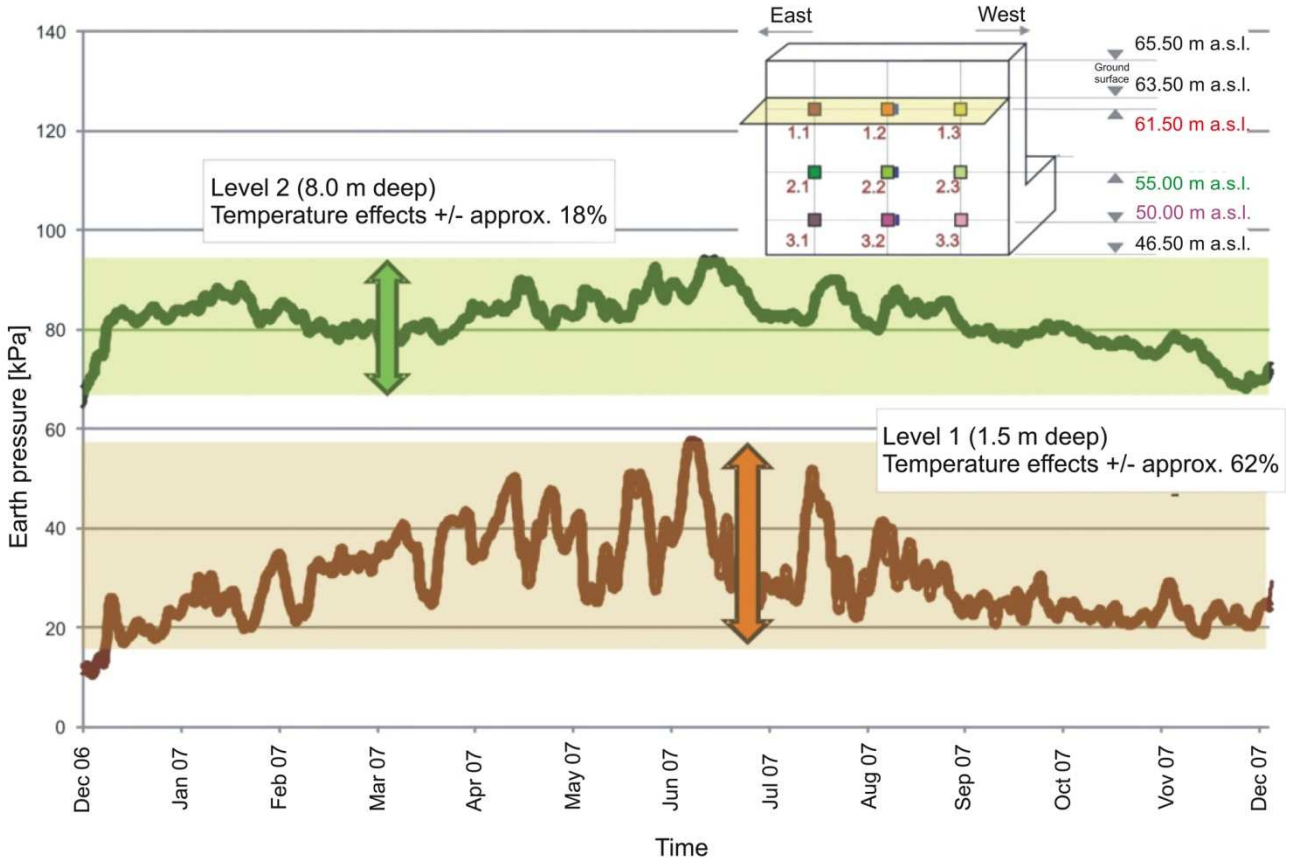

Figure 15: Measured earth pressure at different measuring levels (mean values) in 2007

7.3.2 Effects caused by lock operation

The second major cause of earth pressure changes is the influence of lock operation with fluctuating water loads inside the chamber. In Figure 16 a, the results during the test lock flooding are presented. The test provides clear water loading conditions. Since the test flooding has been carried out in the months of July and August 2008, the water loading is superimposed on the corresponding summer temperatures. However, temperature effects are of minor influence during this period because the changes in long-term temperature are small and the earth pressure measurements were carried out around the same time every day. As expected, the largest earth pressure variations occur on the first measurement level with about 35 kPa. The measured earth pressures in 2009 during normal lock operation show the same magnitude (Fig. 16 b).

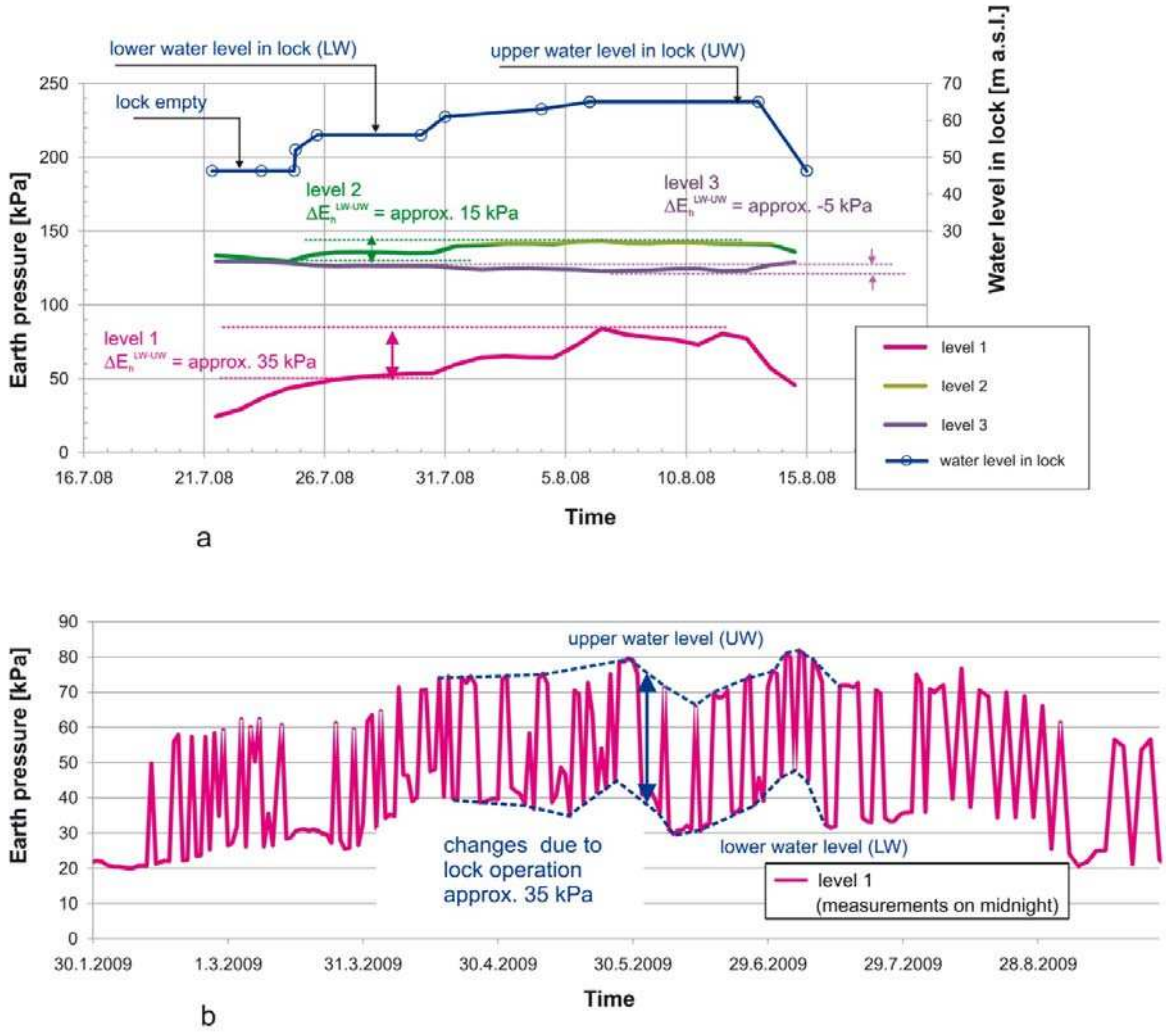

Figure 16: Measured earth pressure (a – during the test flooding, b – during lock operation)

7.3.3 Comparison of earth pressure measurements with finite element simulations

Finite element simulations were performed to examine the distribution of measured earth pressure. Fig 17a represents the measured and computed results for the dewatered and the water-filled construction pit before the lock was in operation. The graph shows a non-classical distribution of earth pressure over depth with rather low values on level 3.

To model the loading history accurately the photographic documentation of the installation of the earth pressure cells and the backfill process was evaluated. The pictures revealed that the backfill in the area of the earth pressure cells was occasionally placed later and in different ways than in the neighbouring areas. To simulate this effect a locally softer backfill (see Fig. 17 on the left) was modelled leading to a redistribution of earth pressure. In addition to this non-uniformity of the backfill some silo effect (the distance between the lock and the diaphragm wall is only 16,5 m for an excavation depth of more than 18 m) explains the small values of the measured earth pressure on level 3.

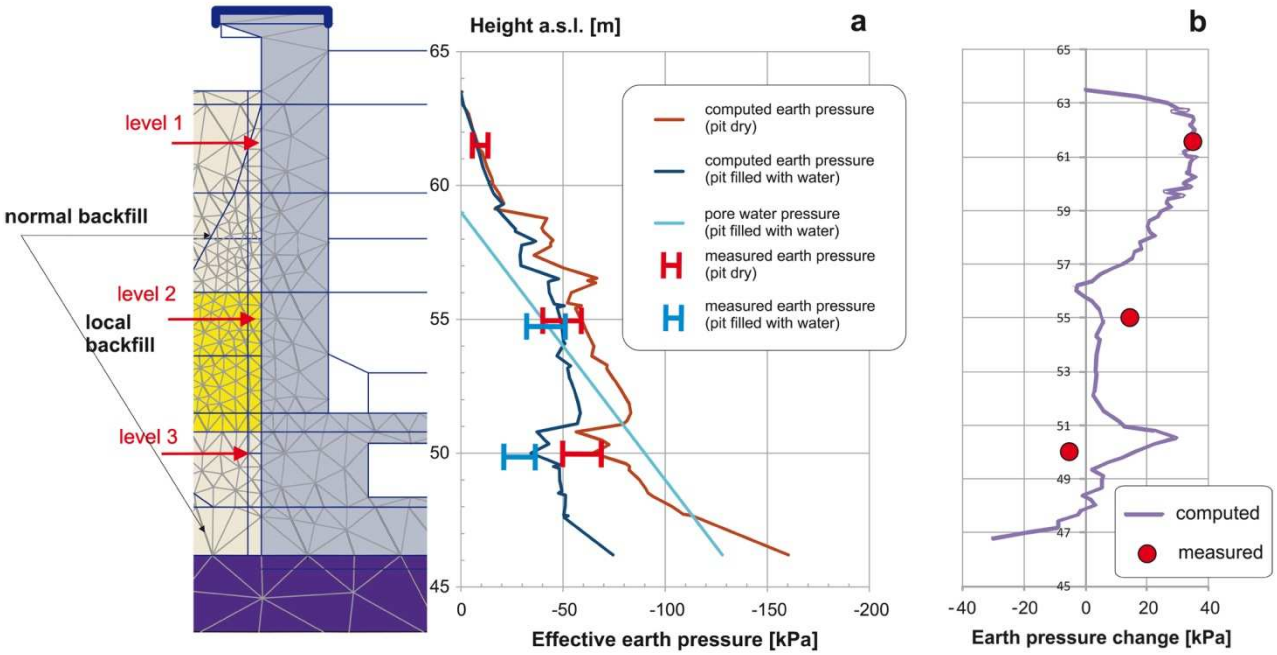

Figure 17: Computed and measured earth pressure distribution (a - lock empty, b - Changes in earth pressure due to water loading in lock)

In Fig. 17 b the changes in earth pressure due to water level changes inside the lock chamber (from the lower to the upper water level) are presented. Following the

deformation characteristics of the U-frame lock structure during the lock water filling phase a concentration of additional earth pressure on the upper part of the lock wall can be observed, whereas the lowest measured level shows a small relief. The computations are in fairly good agreement with the measurements.

8 Conclusions

For the construction of the new southern Sülfeld Lock, a comprehensive geotechnical and geodetic measuring concept had to be designed and implemented due to difficult geotechnical conditions and deformation-sensitive neighbouring structures. This concept involved measurements of deformations, anchor forces, strut forces, earth pressures and the groundwater potential. The conclusions gained from the analysis of those measurements refer on ways how to perform the different measurements and to the finite element modeling of the critical areas of the project:

- The inclinometer measurements at NQ 3 showed that initial readings need to be performed early. This is the only way to determine the total deformation. If this is not possible due to particular construction conditions, the condition of the structure should at least be precisely documented at the time of the initial reading. In general, a complete documentation of the installation or, if needed, of the modification of the measuring systems is important as well as frequent reports of the construction progress with focus on the cross sections. Additional photographic documentation may be very helpful for the interpretation of the results.

- Temperature-induced deformation and resulting constraint play an important role for the forces measured in the struts supporting the retaining wall close to the bridge abutment as well as for measurements of earth pressure at the finished lock. As for struts, (at least short-term) effects of temperature changes can be reduced significantly through thermal insulation. In the design of lock chamber walls, they are taken into account in the form of additional earth pressure which is estimated using finite element computations.

- In the case of the Sülfeld lock, but also for many other projects, there is much less information on the soil properties of the new backfills, which interact with the new structures, compared to the soil present on the site. In order to evaluate the behaviour of new structures, the geotechnical properties of the new fill should also be sufficiently examined.

- To predict future deformation, comprehensive finite element calculations were performed during the planning stage and during the implementation stage. Thanks to this approach, it is possible to continuously calibrate the model according the measuring results, which improves predictions for the following construction phases. Moreover, modifications during the implementation phase and unexpected events can be taken into account in the adaptation of the model and their impact can be estimated quantitatively.

- The measured deformation of the bridge abutment was compared to the calculated results under the consideration of various constitutive laws. The hardening soil model with small-strain stiffness (HSsmall) generated the best results.

- The analysis of the extensometer measurements at NQ 4 showed that a realistic deformation history can only be calculated if consolidation effects are taken into account. The simulation of geological pre-loading is important as well.

References

[1] **Saathoff, J., Schwab, R**.: Anwendung der Finite-Elemente-Methode (FEM) beim Entwurf der neuen Schleuse Sülfeld Süd, *Baugrundtagung in Leipzig, 2004*

[2] **Neumann, S**.: Messtechnische Überwachung beim Bau der neuen Schleuse Sülfeld Süd, *Kolloquium Ingenieurvermessung im Bauwesen der WSV, Bundesanstalt für Gewässerkunde, Koblenz, 2009*

[3] **Benz, T**.: Small-strain stiffness and its numerical consequences. *Institut für Geotechnik Universität Stuttgart, Heft 55, 2006*

[4] **Schwab R., Benz T., Vermeer P**.: An accompanying small-strain model for a large excavation, *Proc. XIV European Conf. on Soil Mechanics and Geotechnical Engn., Madrid 2007*

Authors

Dipl.-Ing. Oliver Stelzer & Dr.-Ing. Radu Schwab

Bundesanstalt für Wasserbau, Kußmaulstr. 17, 76187 Karlsruhe, Germany

E-mail: oliver.stelzer@baw.de

Dipl.-Ing. Sven Neumann

Neubauamt für den Ausbau des Mittellandkanals, Nikolaistr. 14/16, 30159 Hannover, Germany